Solid State Communications 151 (2011) 1336–1339

Contents lists available at SciVerse ScienceDirect

Solid State Communications

journal homepage: www.elsevier.com/locate/ssc

Enhanced nonlinear current–voltage behavior in Au nanoparticle dispersed $CaCu_3Ti_4O_{12}$ composite films

Cong Chen [a,b], Can Wang [b], Tingyin Ning [b], Heng Lu [b], Yueliang Zhou [b,*], Hai Ming [a], Pei Wang [a], Dongxiang Zhang [b], Guozhen Yang [b]

[a] Anhui Key Laboratory of Optoelectronic Science and Technology, University of Science and Technology of China, Hefei, Anhui, 230026, PR China

[b] Beijing National Laboratory for Condensed Matter Physics, Institute of Physics, Chinese Academy of Sciences, Beijing 100190, PR China

ARTICLE INFO

Article history:
Received 14 March 2011
Received in revised form
9 June 2011
Accepted 17 June 2011
by P. Sheng
Available online 24 June 2011

Keywords:
A. Perovskite oxides films
C. Double Schottky barrier
D. Nonlinear *I–V* behavior

ABSTRACT

An enhanced nonlinear current–voltage behavior has been observed in Au nanoparticle dispersed $CaCu_3Ti_4O_{12}$ composite films. The double Schottky barrier model is used to explain the enhanced nonlinearity in *I–V* curves. According to the energy-band model and fitting result, the nonlinearity in Au: CCTO film is mainly governed by thermionic emission in the reverse-biased Schottky barrier. This result not only supports the mechanism of double Schottky barrier in CCTO, but also indicates that the nonlinearity of current–voltage behavior could be improved in nanometal composite films, which has great significance for the resistance switching devices.

1. Introduction

$CaCu_3Ti_4O_{12}$ (CCTO) has attracted great attention in recent years since it was reported as a giant dielectric constant material in 2000 [1] which indicates its potential application in devices based on its dielectric properties. Besides its high permittivity, many efforts have been devoted to study its current–voltage characteristics [2–5]. The strong nonlinear current–voltage behavior was observed in its bulk material with the nonlinear coefficient about 900 [2] which may lead to potential applications in resistance switching devices. Some researchers attributed these properties to interfacial polarization effect [6], the internal boundary layer capacitance effect, and the grain boundary effect [7–12]. Up until now, the origin of high dielectric constant and strong nonlinear *I–V* behavior has not been fully understood. Zang et al. proposed that the *I–V* nonlinearity in CCTO was due to the double Schottky barriers (DSB) formed at the grain boundaries because of the appearance of negative charge sheet [11]. If it is so, the nonlinearity of CCTO could probably be enhanced if it is dispersed by metal nanoparticles which could result in the Schottky barrier at the interface of metal/CCTO.

It is useful to fabricate CCTO thin films with high nonlinear coefficients which could be widely used as resistors or varistors for surge protection, both in electronic circuits and in power systems. However, the current–voltage (*I–V*) nonlinearity of CCTO films is much weaker than that of its bulk material [5]. In order to verify the DSB mechanism in CCTO and enhance the nonlinearity of oxide films, pure CCTO and Au nanoparticle dispersed CCTO (Au: CCTO) composite films were prepared by pulse laser deposition (PLD), and an enhanced nonlinear *I–V* behavior was observed in these composite polycrystalline films with different Au volume fraction. Referring to the DSB model in CCTO [11], the origin of the enhanced nonlinearity is attributed to the double Schottky barriers formed at the interfaces between Au nanoparticles and CCTO.

2. Experimental details

A series of pure CCTO and Au: CCTO polycrystalline films with different Au volume fraction were prepared on MgO (100) substrates by pulse laser deposition (PLD) at 800 °C under an oxygen pressure of 10 Pa. During the deposition process, Au and CCTO targets were alternately ablated by the pulsed laser beam and deposited onto the substrates, so the Au nanoparticles were dispersed into whole CCTO films randomly. The thicknesses of the CCTO and Au: CCTO films were measured to be 300 nm by a surface profile measuring system (DEKTAK, USA). Served as the electrodes, two ITO films with length of 3 mm and width of 1 mm were deposited on each film through a mask at 500 °C under 3×10^{-3} Pa.

* Corresponding author. Fax: +86 10 82649356.
E-mail address: ylzhou@aphy.iphy.ac.cn (Y. Zhou).

0038-1098/$ – see front matter © 2011 Elsevier Ltd. All rights reserved.
doi:10.1016/j.ssc.2011.06.024

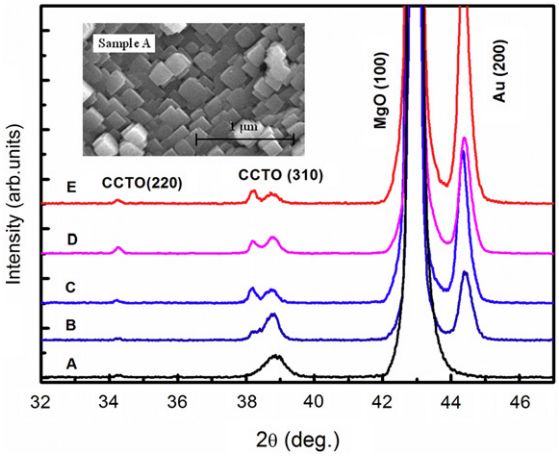

Fig. 1. XRD spectra of the pure CCTO and Au: CCTO films on MgO (100). The inset shows the surface morphology of the pure CCTO film observed by SEM.

The crystalline structure and crystallographic orientation of the CCTO and Au: CCTO films were analyzed by X-ray diffraction (XRD) with Cu Kα radiation at 1.54 Å. The microstructure and surface morphology of the samples were observed by using scanning electron microscopy (SEM), while the chemical compositions of the films were measured by the energy dispersive X-ray analysis (EDAX). The values of current, corresponding to different intensity of electric field, were recorded by Keithley 2400 SourceMeter. Every single I–V curve was measured three times to ensure that the experimental data were reliable. It should be pointed out that the value of current was below 15 μA during all the measurements, so the thermal effect can be ignored.

3. Result and discussion

Fig. 1 shows the XRD result of the CCTO and Au: CCTO films on MgO (100) substrates. The pure CCTO film is named as A, and the other four Au: CCTO films were labeled as B, C, D, and E in terms of the increase in Au volume fraction. The CCTO diffraction peak mainly consists of CCTO (220) and (310) peaks though the (220) peak is quite feeble, which represents the lattice structure of CCTO to be polycrystalline. After being dispersed with Au nanoparticles, the Au (200) peak appears and the CCTO (310) peak splits, which means that the dispersed Au nanoparticles would strongly frustrate the crystal growth of CCTO. This phenomenon probably arises from the stress exerted on CCTO nanocrystals induced by Au nanoparticles [13]. The average size of Au nanoparticles is about 20 nm calculated from the full width at half maximum (FWHM) of the Au (200) peak.

The SEM images of the pure CCTO and Au: CCTO films are shown in the inset of Figs. 1 and 2, respectively. The cubic crystal grain of the pure CCTO film can be observed clearly due to its body-centered cubic crystal structure [14]. However, the crystal grain of CCTO changes abruptly after being dispersed with Au nanoparticles, which is consistent with the result of XRD. The Au volume fraction of the four Au: CCTO films are measured to be 18%, 22%, 27% and 31%, corresponding to samples B, C, D and E, respectively, based on the analysis of EDAX. It can be seen that there are numerous nanoparticles dispersed among the irregular CCTO grains, and the number of nanoparticles becomes larger with the increase in Au volume fraction. Estimated from the result of SEM, the size of the nanoparticles is about tens of nanometers, which is closed to the calculation result according to the XRD peak of Au nanoparticles. So, it is reasonable to conclude that these nanoparticles observed by SEM are the dispersed Au particles.

The current–voltage properties of CCTO and Au: CCTO films were investigated at room temperature as shown in Fig. 3. As can be seen, the nonlinear I–V characteristics were observed in all the five samples. Calculated from the slope at different values of the electric field, the resistivity of the films decreases as the electric field becomes larger. The value of resistivity at the same electric field decreases when the volume fraction of Au nanoparticles increases. In order to establish that the nonlinearity was not caused by the contact of ITO and CCTO, the I–V behavior of In/CCTO/ITO sandwiched film sample was measured, and no rectifying characteristic was observed. This result indicates that it can be considered as an Ohmic contact at the interface of CCTO/ITO.

In general, the I–V correlation for a varistor can be expressed by [15]

$$I = KV^{\alpha} \tag{1}$$

where K is a constant related to the electrical resistivity of the material. α is the nonlinear coefficient, which indicates the nonlinearity of I–V characteristics. Fit by Eq. (1), the nonlinear

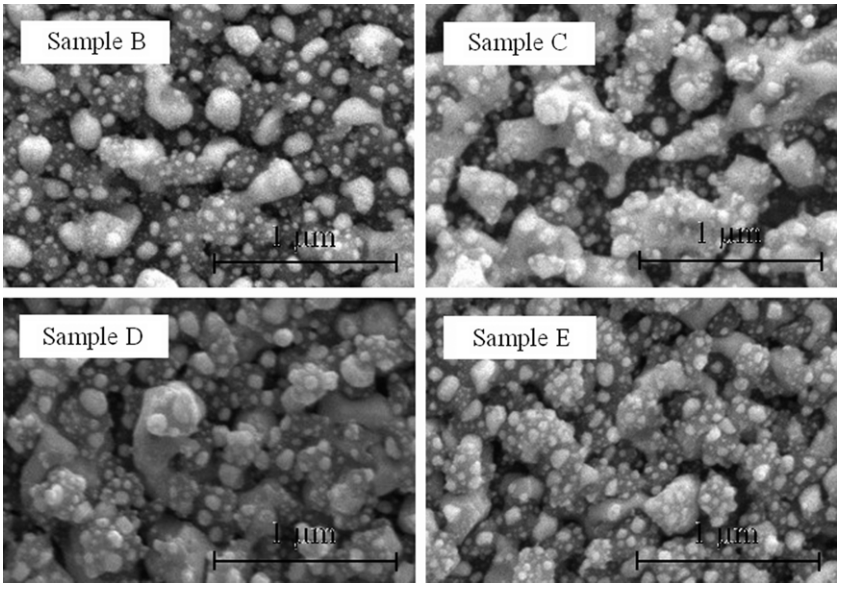

Fig. 2. The surface morphology of the four Au: CCTO films with different Au fraction volume observed by SEM. The value of the scale is 1 μm.

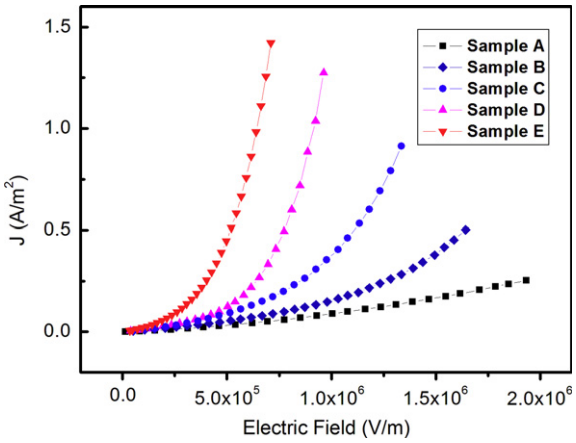

Fig. 3. The *I–V* characteristics of the pure CCTO and Au: CCTO films measured at room temperature.

coefficient of the samples A, B, C, D and E is about 1.5, 2.1, 2.7, 3.9 and 3.1, respectively. It can be seen that, the nonlinearity of Au: CCTO films can be enlarged by 2–3 times than that of pure CCTO films.

So far, several leakage current mechanisms have been reported to explain the nonlinear current–voltage behavior in CCTO, such as the Poole–Frenkel emission [16], Schottky emission [16] and grain boundary effect [2,11], etc. In our experiments, the enhanced nonlinear *I–V* behavior is attributed to double Schottky barriers formed at the interface of CCTO/Au, supporting the validity of the DSB model [11].

Because CCTO has been thought to be n-type conduction by electrons due to oxygen vacancies or the substitution of Ti in the Cu sites [17], it can be considered as an n-type semiconductor with high resistivity. So it is reasonable to suppose that there are numerous semiconductor–metal–semiconductor structures composed of Au grains sandwiched between the surfaces of n-type semiconductive CCTO grains. The band gap energy E_g of the CCTO film has been obtained to be about 3.25 eV calculated from the transmittance spectrum of CCTO films. The values of electron affinity for CCTO and Au (χ(CCTO) = 3 eV [18], Φ(Au) = 5.3 eV [19]) are taken to construct the band structure.

According to the discussion above, the non-biased and biased energy-band diagrams of double Schottky barriers are shown in Fig. 4. In order to clarify the *I–V* behavior in such DSB, it is necessary to discuss the conduction mechanisms in three different regions of the energy-band model. In region I, the conduction mechanism is governed by a forward-biased Schottky barrier. And in region II, the electron can move freely inside the metal under the applied voltage, while the conduction mechanism in region III is governed by a reverse Schottky barrier. Since the reverse-biased Schottky barrier plays a dominating role in the series connection of back-to-back rectifying barrier, the conduction process in region I has no strong effect on the nonlinear *I–V* curves. Judging from these discussions, it is reasonably considered that the conduction mechanism is governed by reverse Schottky barriers in the enhanced nonlinear *I–V* behavior of Au: CCTO films.

So far, the conduction mechanism explained by the DSB model in Au: CCTO film is still not enough to be convincing. The microstructure of Au: CCTO films seems to be porous from the surface SEM figures. It is well known that the porous structure affects the varistor behavior. In order to make out the dominating conduction mechanism in our sample, *the I–V curves are fitted by using the current–voltage behavior of the reverse-biased Schottky barrier*.

For a reverse-biased Schottky barrier, there are three conduction mechanisms: (1) thermionic emission, (2) thermally assisted field emission and (3) field emission. The current–voltage characteristics of the three mechanisms can be expressed as follows [20]:

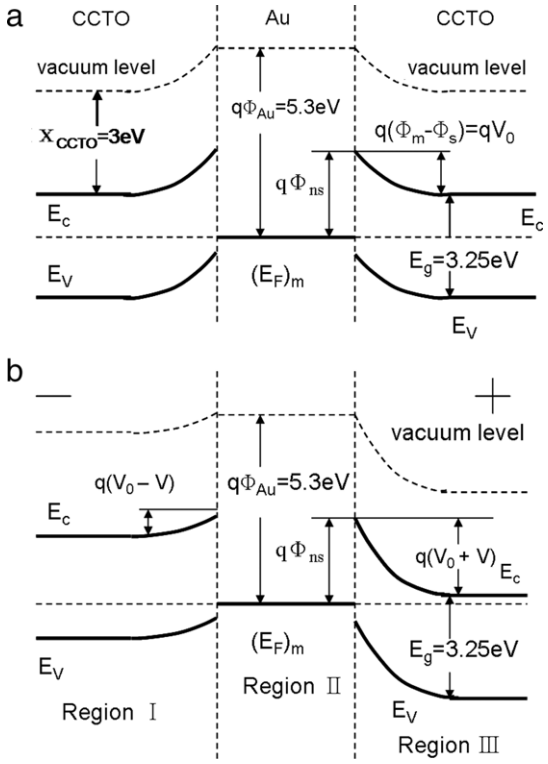

Fig. 4. (a) The energy-band model of the double Schottky barrier under no bias. (b) the energy band of the double Schottky barrier under applied bias.

Thermionic emission:

$$J = AT^2 \exp\left(-\frac{E_B - \beta E^{1/2}}{kT}\right) \tag{2}$$

where $\beta = (q^3/4\pi\varepsilon)^{1/2}$, E_B is the electric barrier height formed at the interface region.

Thermally assisted field emission:

$$J = J_{STF} \exp(-E/\varepsilon'). \tag{3}$$

Field emission:

$$J = J_{SF} \exp\left[-\frac{2E_B^{3/2}}{3E_{00}(E_{00} - E)^{1/2}}\right]. \tag{4}$$

As shown in Fig. 5, the plots, ln(J) vs. $E^{1/2}$, show regions with straight fits to the data of all the five samples at high electrical field, which means that the dominating conduction mechanism is thermionic emission in the conduction of Au: CCTO films, *but not the surface effect resulting from the porous structure*. It should be noticed that the fit results of β and E_B should be the value of the series connection of back-to-back rectifying barriers, different from the single reverse-biased Schottky barrier. The reason why the *I–V* curve of pure CCTO film can also be explained by the DSB due to the appearance of the negative charge sheet at the interface between CCTO grains [11,21]. Concluded from the discussion above, the origin of the enhanced nonlinear *I–V* behavior can be contributed to the introduction of numerous double Schottky barriers due to the dispersed Au nanoparticles. It can be expected that the nonlinearity of *I–V* curves will be enhanced as the Au volume fraction increases because the number of DSB is related to Au concentration, which is consistent with the result of samples

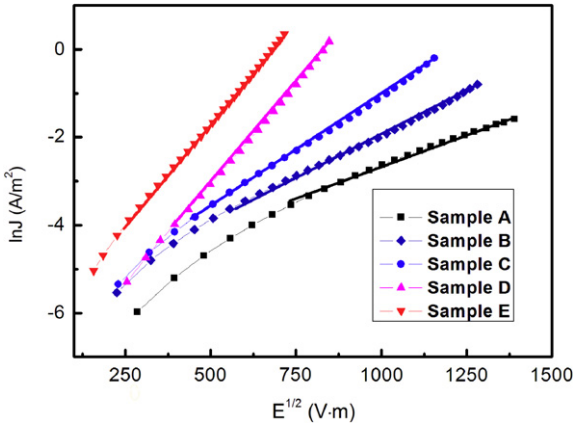

Fig. 5. The relationship between $\ln(J)$ and $V^{1/2}$, which shows regions with straight fits to the data of all the five samples.

A–D. The reason for the decrease phenomenon of nonlinearity in sample E is that the Au volume has been larger than the percolation limit [22,23].

4. Conclusions

In summary, enhanced nonlinear I–V characteristics have been observed in Au: CCTO films. Not only the validity of the DSB model in CCTO is verified, but also a new method is proposed to enhance the nonlinearity of perovskite oxide films, as long as there are Schottky barriers at the interfaces of metal and perovskite oxide. It can also be expected that the nonlinearity could be improved if metal nanoparticles are dispersed more uniformly, which could enhance the percolation limit.

Acknowledgments

This work was supported by the National Key Basic Research Program of China (Grant No. 2011CB301802) and the National Natural Science Foundation of China (Grant No. 10874226).

References

[1] M.A. Subramanian, D. Li, N. Duan, B.A. Reisner, A.W. Sleight, J. Solid State Chem. 151 (2000) 323.
[2] S.Y. Chung, I.D. Kim, S.L. Kang, Nat. Mater. 3 (2004) 774.
[3] Y.H. Lin, J.N. Cai, M. Li, C.W. Nan, Appl. Phys. Lett. 88 (2006) 172902.
[4] B. Cheng, Y.H. Lin, Y.C. Yuan, J.N. Cai, W.C. Nan, X. Xiao, J.L. He, J. Appl. Phys. 106 (2009) 034111.
[5] Y.W. Li, Y.D. Shen, Z.G. Hu, F.Y. Yue, J.H. Chu, Phys. Lett. A 373 (2009) 2389.
[6] L. Wu, S. Zhu, S. Park, S. Shapiro, G. Shirane, Phys. Rev. B 71 (2005) 014118.
[7] L. Chen, C.L. Chen, Y. Lin, Y.B. Chen, X.H. Chen, R.P. Bontchev, C.Y. Park, A.J. Jacobson, Appl. Phys. Lett. 82 (2003) 2317.
[8] T.T. Fang, H.K. Shiau, J. Am. Ceram. Soc. 87 (2004) 2072.
[9] I.D. Kim, A. Rothschild, H.L. Tuller, Appl. Phys. Lett. 88 (2006) 072902.
[10] D.C. Sinclair, T.B. Adams, F.D. Morrison, A.R. West, Appl. Phys. Lett. 80 (2002) 2153.
[11] G.Z. Zang, J.L. Zhang, P. Zheng, J.F. Wang, C.L. Wang, J. Phys. D 38 (2005) 1824.
[12] T.B. Adams, D.C. Sinclair, A.R. West, Phys. Rev. B 73 (2006) 094124.
[13] J. Li, X.L. Wu, D.S. Hu, Y.M. Yang, T. Qiu, J.C. Shen, Solid State Commun. 131 (2004) 21.
[14] B. Bochu, M.N. Deschizeaux, J.C. Joubert, A. Collomb, J. Chenavas, M. Marezio, J. Solid State Chem. 29 (1979) 291.
[15] D.R. Clarke, J. Am. Ceram. Soc. 82 (1999) 485.
[16] G.W. Pabst, L.W. Martin, Y.H. Chu, R. Ramesh, Appl. Phys. Lett. 90 (2007) 072902.
[17] L.T. Mei, H.I. Hsiang, J. Am. Ceram. Soc. 91 (2008) 3735.
[18] P. Fiorenza, R. LoNigro, A. Sciuto, P. Delugas, V. Raineri, R.G. Toro, M.R. Catalano, G. Malandrino, J. Appl. Phys. 105 (2009) 061634.
[19] W.M.H. Sachtler, G.J.H. Dorgelo, A.A. Holscher, Surf. Sci. 5 (1966) 221.
[20] F.A. Padovani, R. Stratton, Solid-State Electron. 9 (1966) 695.
[21] K. Eda, J. Appl. Phys. 49 (1977) 2964.
[22] N. Lebovka, M. Lisunova, Y.P. Mamunya, N. Vygornitskii, J. Phys. D: Appl. Phys. 39 (2006) 2264.
[23] S. George, N.I. Santha, M.T. Sebastian, J. Phys. Chem. Solids 70 (2009) 107.